Impedance-Based Battery Management System for Safety Monitoring of Lithium-Ion Batteries

Bliss G. Carkhuff, Plamen A. Demirev, and Rengaswamy Srinivasan

***Abstract*—Multifrequency impedance measurements have been recognized as a technique for the monitoring of individual cells in lithium-ion (Li-ion) batteries. However, its practical introduction for battery management has been slow, mainly due to added size and larger operating power requirements. Here, we describe a small, low-power, multifrequency (1–1000 Hz) impedance-based battery management system (BMS) for multicell batteries of varying capacities. This BMS ensures battery safety and efficiency by tracking and acting on emerging mismatches and other electrical and thermal abnormalities in each individual cell without adding cost, volume, weight, and power, compared to conventional BMSs. Multicell batteries face a unique problem that single-cell Li-ion batteries do not: mismatching of one or more cells is detrimental to the safety and efficiency of the entire battery. Thus, cell matching is an important first step required for safe operation of multicell Li-ion batteries. Cell mismatch can occur due to battery overdischarge, overcharge, internal and external shorts, etc., or even when leaving a battery unused for an extended period (calendar aging). Predicting a mismatch is essential for a battery's thermal safety and electrical efficiency. Conventional BMSs typically monitor cell voltages and surface temperature. However, these measurements and related protocols have not succeeded in ensuring battery safety or improving efficiency. Data for batteries with intentionally calendar-aged and overdischarged cells convincingly demonstrate that such BMSs cannot identify cell mismatches and emerging failures. In contrast, the impedance-based BMS, described here, tracks, identifies, and acts on changes in the internal state of each cell continuously in real time, including battery charging, discharging, and at rest.**

***Index Terms*—Anode impedance, cathode impedance, cell internal temperature, cell matching in batteries, electrolyte resistance, lithium-ion battery, real-time monitoring, sensorless monitoring internal states.**

I. Introduction

In a multicell lithium-ion (Li-ion) battery, all cells should be "matched" for best battery performance. Most battery safety and qualification standards require that a battery should be built using only matched cells. Yet, little attention is paid to ensure that all cells remain matched throughout the battery lifecycle.

Normal operations as well as calendar aging (battery being only stored) drive the cells within the battery toward mismatch. Permanent or intermittent external short of even a single cell in a multicell battery also causes cell mismatch.

Other factors may include nonuniform heating of cells, internal shorts, and faulty chargers that may cause one or more cells to overcharge. In order to ensure safety, a battery management system (BMS) should identify mismatched cells throughout the battery lifecycle. In practice, cell matching is performed only when a battery is manufactured, but not afterward. Once the battery is installed, in most cases, cells are rarely monitored for cell matching (excluding cell voltage matching during charging). Typically, equipment that uses Li-ion batteries has a BMS that only monitors cell voltage $E_{\rm cv}$ and cell surface temperature $T_{\rm surf}$. Decades of emphasis on requiring voltage and surface temperature monitoring for battery safety has created "gold" standards for BMS [1], and practical tools that monitor faults in $E_{\rm cv}$ and $T_{\rm surf}$ sensors [2]. Some BMS also monitor ampere-hour capacity (Ah-capacity), and much less often internal impedance $R_{\rm s}$ at a single frequency, typically 1 kHz [3], [4].

Until now, there has been no BMS that monitors internal impedance at multiple frequencies. In order to fully characterize the impedance, the BMS should be able to accurately measure in-phase and quadrature (i.e., real and imaginary) components over three decades, typically between 1 and 1000 Hz [5], [6]. By monitoring both amplitude and phase shift at multiple frequencies, the BMS will fully characterize the impedance of the anode, cathode, and the electrolyte. The design requirements of such an impedance-measurement system are complex and have so far limited the inclusion of a "true" impedance meters. To prevent interfering with the equipment that the battery is powering, such a BMS should not add more than a few mV ac voltage between the cell terminals. A BMS with a single-frequency-impedance-meter, the only type described so far [3], [4], essentially only monitors $E_{\rm cv}$, $T_{\rm surf}$, and the electrolyte resistance, R_s.

A typical BMS uses $E_{\rm cv}$ data to ensure that the cells do not exceed preset upper and lower limits during charging and discharging, respectively. Ah-capacity and R_s monitoring is not directly related to safety, although frequently used to identify capacity matching, loss of capacity, and power. A BMS that monitors only the maximum and minimum $E_{\rm cv}$, single frequency impedance, battery's Ah-capacity, and $T_{\rm surf}$ of a few

Manuscript received March 17, 2017; revised July 3, 2017, August 1, 2017, October 13, 2017, and November 20, 2017; accepted December 8, 2017. Date of publication January 5, 2018; date of current version April 2, 2018. This work was supported by the Independent Research and Development Program of the Johns Hopkins University Applied Physics Laboratory. *(Corresponding author: Rengaswamy Srinivasan.)*

The authors are with the Johns Hopkins University Applied Physics Laboratory, Laurel, MD 20723 USA (e-mail: bliss.carkhuff@jhuapl.edu; plamen.demirev@jhuapl.edu; rengaswamy.srinivasan@jhuapl.edu).

Color versions of one or more of the figures in this paper are available online at http://ieeexplore.ieee.org.

Digital Object Identifier 10.1109/TIE.2017.2786199

cells, may not identify mismatched cells. Test data presented below show that monitoring only $E_{\rm cv}$ and $T_{\rm surf}$ does not ensure adequate electrical and thermal safety. Even though battery safety standards routinely recommend the use of cell parameters such as $E_{\rm cv}$, Ah-capacity, $T_{\rm surf}$, and R_s to identify mismatched cells [7], [8], the data presented below show that in a multicell Li-ion battery $E_{\rm cv}$, $T_{\rm surf}$, Ah-capacity and R_s values alone do not indicate cell mismatch.

In this paper, we demonstrate that multifrequency impedance data (real and quadrature covering three decades of frequency domain) can be correlated reliably to evolving cell mismatches under three common scenarios: cycle life aging, calendar life aging, and overdischarge and overcharge. We also describe a new and practical BMS that in addition to the conventional $E_{\rm cv}$ monitor contains a multifrequency impedance meter. Our impedance-based BMS has small size (10 × 10 cm), low power demand (6 V; 0.75 A dc), and standalone operation (no need for an external processor to manage the battery and direct commands to external controls such as switches and relays).

II. Test Batteries and Test Setup

We used five different types of Li-ion batteries in our tests. For all batteries, new cells, rated to 5.3 Ah capacity, were selected (Swing 5300 model, Boston Power, Boston, MA, USA). The new cells were cycled twice between 2.7 and 4.2 V at C/4-rate, brought to 50% state of charge (SoC), rested overnight at room temperature before screening for matching and making the batteries. Only cells that matched within 3 mV, and in multifrequency impedance within ±0.5%, and identical in Ah-capacity were selected for assembling batteries. Within one day after the cell screening and selection, we assembled one three-cell battery, one six-cell battery and reserved two individual cells for abuse (overdischarge and overcharge) tests. Tests on the three-cell battery started within one day after assembly. The six-cell battery and the two spare cells were stored under ambient conditions for six months before testing. In addition, we also report one set of data on electrolyte resistance (see Fig. 4) collected using three matched individual cells (Swing 4400 model, Boston Power). The cells were fully ventilated from all sides to prevent unbalanced thermal constrains. The cells were separated by 5 mm air gap from each other. The battery was raised 5 mm above the resting table, and its top was fully open to air to minimize cell-to-cell heat transfer.

Definitions of "normal," "bad," and "matched cells": a new cell is "normal" if 1) its Ah-capacity determined at C/4 rate discharge–charge cycle is the same or better than the nameplate capacity and 2) its internal real and quadrature impedances at 1 kHz, 10 Hz, and 1 Hz all match within ±0.5% of multiple cells from the same lot. An aged cell is "normal" if 1) its Ah-capacity determined at C/4 rate discharge–charge cycle follows a linear decay that does not exceed 20% of its nameplate capacity at the manufacturer-specified end of life and 2) its internal real and quadrature impedances at 1 kHz, 10 Hz, and 1 Hz all match within 5% of the new normal cell. A cell is "bad," within the context of this work, if it has been overdischarged ($E_{\rm cv}$ dropping almost to zero volt) or overcharged ($E_{\rm cv}$ reaching few hundred millivolts above 4.2 V) at least once. Cells are "matched" if their voltages are within ±5 mV at full charge, Ah-capacities are within ±5 mAh, and their impedances have a ±0.5% at each of the following frequencies: 1 kHz, 100 Hz, 10 Hz, and 1 Hz.

Impedance measurements were made using two different instruments: 1) a commercial bench-top instrument (Solartron Frequency Response Analyzer, SI1250, and Electrochemical Interface, SI1287) and 2) an impedance-based BMS designed by us (described in detail in Section V). Both were multifrequency capable, in the 1–1000 Hz range, where the impedance data over that range yielded complete information about the cell anode impedance, cathode impedance, electrolyte resistance, anode temperature, cathode temperature, and electrolyte temperature [11], [12], [20]–[23]. Both were capable of measuring amplitude and phase at each frequency. Our impedance-based BMS also monitored cell voltage of each cell in the battery. We used Arbin Instruments Model BT2000 for discharge–charge cycling and monitoring surface temperature.

Though the operating principles of the impedance-based BMS are described in detail in Sections V and VI, we provide here a brief description of the procedure involved in measuring a cell's internal temperature ($T_{\rm int}$). $T_{\rm int}$ refers to the temperature of different components within the cell, for example, the anode, cathode, and electrolyte. The impedance of each component has different behavior at different frequency ranges [11], [21], the respective impedance values can be measured for at least one frequency within each range. After the frequencies are identified, the impedance-based BMS must be calibrated for $T_{\rm int}$, using the procedure described in Section V.

III. Cell Voltage, Surface Temperature, and Electrolyte Resistance Data for Matched and Mismatched Cells

Using new, cycle-aged, calendar-aged, or overdischarged cells, we first highlight the shortcomings of cell voltage, surface temperature, and electrolyte resistance monitors to detect and predict cell mismatch. In Section V, we compare these data with our impedance-based BMS data. These results highlight that bad and normal cells are nearly identical in their $E_{\rm cv}$ and $T_{\rm surf}$ values, while high-frequency impedance is concurrently influenced by electrolyte temperature, cell aging and changes in Li^+ concentration.

A. Cell Voltage Monitor

$E_{\rm cv}$ monitoring is a commonly incorporated feature in conventional BMS. Its main role in a BMS is to ensure that no cell in the battery exceeds preset upper and lower limits, respectively. At open circuit, $E_{\rm cv}$ represents the difference between Nernst thermodynamic potentials of the anode and the cathode. During current flow (when charging or discharging), $E_{\rm cv}$ is dominated by three different polarization effects: activation and diffusion at the anode and the cathode, and resistive drop across the electrolyte, with relatively insignificant contributions from foreign-object-debris (FOD). FOD refers to any nonfunctional material that despite careful cell manufacturing may find its way into the cell. For example, FOD include copper and aluminum particulates from current collectors. FOD can cause internal short circuit, chemical changes induced by overdischarge, and chemical

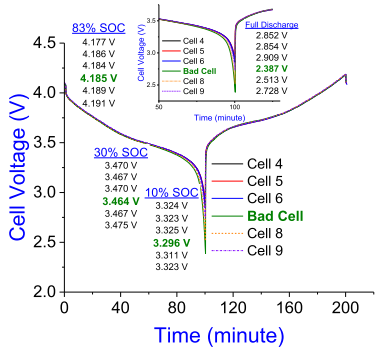

Fig. 1. Individual cell voltages during discharge and charge of a six-cell Li-ion battery containing five matched, calendar-aged cells and one overdischarged cell under one of the multiple discharge–charge cycles. During discharge, the differences in voltage between the six cells were within ±5 mV. The difference between the overdischarged cell and the other five cells is evident only when the battery is fully discharged (inset).

and physical changes after cycle and calendar aging. As a result, E_{cv} of cells with FOD, overdischarge and age abnormalities will be quite similar to those of cells without those abnormalities. FOD, overdischarge, and aging are the main reasons why cells become mismatched; however, cell voltage monitoring alone cannot identify cell mismatch.

The data in Fig. 1 demonstrate that in a six-cell battery with five aged cells and one overdischarged cell, the E_{cv} of all six cells remained close (standard deviation under ±5 mV), down to 30% SoC during discharge, and at all SoC during charge. Only below 20% SoC did the cell voltages start to deviate markedly from each other, with the overdischarged (bad) cell deviating most at full discharge. At full discharge, the bad cell was at 2.387 V, i.e., 313 mV below the manufacturer-recommended 2.7 V limit for the cell, while the voltage of the entire battery reached only its lower limit (16.2 V), falsely suggesting that each cell was at the 2.7 V limit (2.7 V × 6 = 16.2 V). A cell-voltage monitor in a BMS is thus not always capable of identifying mismatched and overdischarged cells, and will miss bad cells discharging far below their recommended limit, which might cause a battery fire [13]. In the two batteries with all new cells and all aged cells, the difference in voltage between the cells remained within ±5 mV through the entire range of charge and discharge (data not shown).

B. Surface Temperature Monitor

We next monitor cell surface temperature T_{surf} in order to identify cell mismatching. Battery voltage (indicating the discharge/charge cycle) and surface temperature variations for one normal and the bad (previously overdischarged) cell in the six-cell battery from Fig. 1 are plotted in Fig. 2. The surface temperatures of the normal and overdischarged cells were virtually identical until the battery was fully drained (at 687 min time point). For a completely drained battery, the surface temperature of the bad cell deviates by no more than one degree from normal cell temperature (24 °C). In other words, surface-mounted temperature sensors can barely discriminate an overdischarged (i.e., mismatched) cell from normal cells. Similarly, for batteries with new and cycle-aged cells, individual cell T_{surf} values were identical to each other (data not shown).

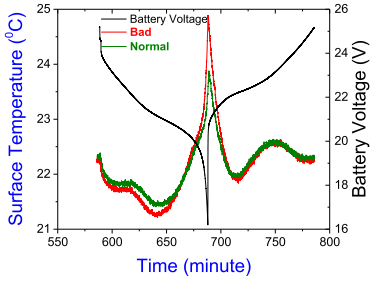

Fig. 2. Surface temperatures of one aged (normal, green) and one overdischarged (bad, red) cell. In Fig. 2 and subsequently (Figs. 3, 5, and 9) the graph in black represents the battery voltage during discharge and charge.

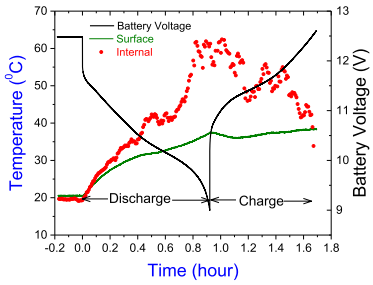

Fig. 3. Surface temperature (green) and internal (anode) temperature (red) of one of the cells in a cycle-aged three-cell battery.

In addition to not being adequate in discriminating bad cells from normal ones, surface-mounted sensors have several more shortcomings. T_{surf} sensors are slow in responding to changes in the discharge currents flowing through the cell [11, Fig. 11], and they cannot identify when the cell is being overcharged [12, Fig. 2]. Furthermore, when a battery is rapidly charged or discharged, T_{surf} values do not indicate impeding damage to the interior of the cell. For example, through the discharge–charge cycle at 1 C rate of a three-cell battery, T_{surf} remained well within 20 °C to 40 °C (see Fig. 3). This temperature range is considered "safe" by most battery safety standards. However, the cell's internal temperature exceeded 60 °C, less than 20° below 80 °C, considered unsafe by most standards.

C. Electrolyte Resistance Monitor

R_s reportedly serves two purposes: 1) to identify a cell's internal temperature [14]–[16]; 2) to estimate cell aging and health [17]. In both cases, R_s is determined from measured cell impedance at a single frequency (typically between 300 Hz and 10 kHz). In that range, the phase shift is either zero, or only slightly negative or positive. R_s monitoring has limited merits, but only when measurements are made for a cell at rest, not when it is (dis)charged. While single-frequency impedance monitoring can estimate cell cycle-life aging, it is valid only if impedance is measured after the cell is rested for extended time at constant ambient temperature (see Fig. 4). Furthermore, R_s can be correlated to the temperature of the electrolyte only if age-induced changes in electrolyte resistance are ignored and no current is flowing through the cell.

For example, Li^+ cations, released into the electrolyte from the anode during discharge, are taken into the cathode; the

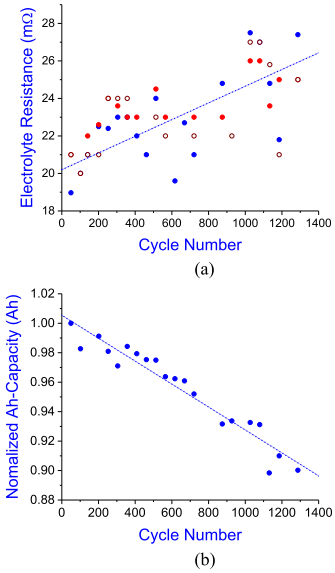

Fig. 4. (a) Effect of cycle life on electrolyte resistance, R_s, in three identical Li-ion cells. The line is a linear fit of the entire data set; and (b) Ah-capacity as a function of cycle life for one of the three cells. The cells are Boston Power Swing 4400 cells that went through 1300 cycles, with a 70% depth-of-discharge per cycle. After every 50 to 100 cycles, the cells were brought to 50% SoC and rested overnight at 20 °C before measuring R_s.

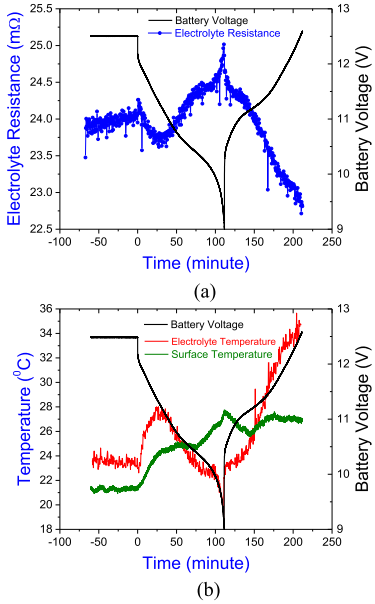

Fig. 5. (a) Electrolyte resistance, R_s of one cell during a single cycle of discharge–charge of a new and matched three-cell battery [same as in Fig. 6(b)]. Both internal temperature and Li^+ ion concentration, $[Li^+]$, are influencing R_s. (b) Internal temperature (red) of the same cell, as inferred by high-frequency impedance [14]–[16], and surface temperature (green) measured using a surface-mounted thermocouple mounted on that cell. The trends in R_s and internal temperatures for the other two cells (not included) are identical to those shown.

opposite process occurs during charge. However, the rates of release and intake, reflecting the anode and cathode reaction kinetics, respectively, differ—the release rate is higher than the intake [18], [19]. The rate differences between the two electrodes result in $[Li^+]$ buildup in the electrolyte. Battery manufacturers optimize $[Li^+]$ in the electrolyte for lowest resistance. However, $[Li^+]$ change during discharge and charge results in a change in electrolyte resistance. In the example shown [see Fig. 5(a)], during cell charge and discharge at C/2-rate, R_s varied between 22.7 and 25 mΩ. This 14% variation between R_s maximum and minimum is comparable to the 30% change observed due to cycle life aging [see Fig. 4(a)]. Therefore, monitoring cell aging from high-frequency impedance data may be feasible only if impedance is measured when the cell is at rest, and care is taken to maintain the cell at the same internal temperature between each measurement [see Fig. 4(a)].

The variation in R_s can be caused by changes in electrolyte temperature as well as changes in $[Li^+]$ in the electrolyte. It is beyond the scope of our work here to identify the proportional contribution to R_s. If impedance measurements are used in estimating electrolyte temperature during charge and discharge, the current-induced changes in $[Li^+]$ will introduce errors in those estimates, as demonstrated in the discrepancy between the cell internal temperature (estimated from high-frequency impedance) and the surface temperature [see Fig. 5(b)]. The changes in T_{surf} [see Fig. 5(b)] are characteristic for this type of Li-ion cell [20]. Compared to T_{surf}, the internal temperature behaved differently—after an initial rise to 28 °C during discharge, it subsequently dropped. The drop in internal temperature is an artifact, best explained by the differences in reaction kinetics between the anode and the cathode and $[Li^+]$ changes during discharge [18], [19].

IV. Impedance Approach to Identify Cell Mismatch

A Li-ion cell is a multicomponent system, consisting of an anode, cathode, electrolyte, separator, and current collectors. Each component reacts differently to temperature and current flows as discussed in detail in a number of publications [11], [12], [20]–[23]. The solid-electrolyte-interphase (SEI) layer is most sensitive to temperature and least sensitive to SoC. Current flow changes SEI layer's temperature, therefore measuring the impedance allows to monitor the cell's anode and cathode temperatures. Low-frequency impedance (10–1 Hz) is influenced by both SoC and internal temperature; however, separating their effects can be challenging. R_s, best identified as high-frequency impedance, is also sensitive to temperature, $[Li^+]$ and cell aging. Thus, a multifrequency impedance meter equipped to measure both phase shift and amplitude is required to discern changes occurring in the anode, cathode, and the electrolyte.

The battery cells used in this study are described in Section II. Fig. 6(a) shows impedance data for three cells in a three-cell battery matched within ±0.5%. At full charge and 50% SoC, the cell voltages matched within 3 mV and the Ah-capacities were nearly identical. Each is a new cell cycled twice between 2.7 and 4.2 V at C/4-rate, brought to 50% SoC, and rested overnight at room temperature before measuring the impedance with a constant amplitude sinusoidal current (25 mA rms).

Fig. 6(b) shows impedance data for each of the six cells in a six-cell battery after aging. The cells (from the same lot as in Fig. 6(a) with identical Ah-capacity and cell voltage) were similarly cycled twice and brought to 50% SoC, and left to rest (age) for six months under ambient conditions. After six months, the six-cell battery was cycled twice, brought to 50%

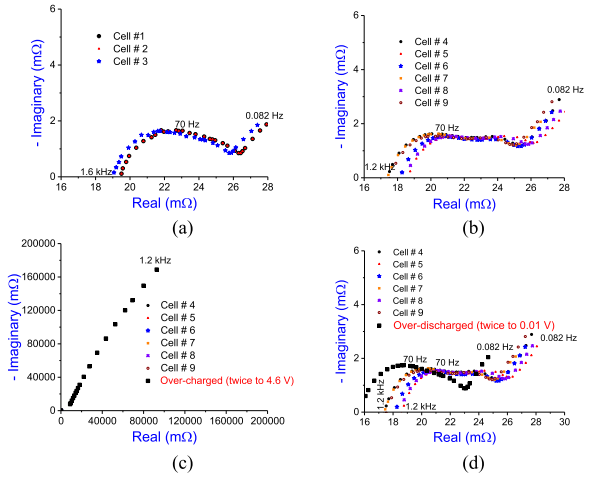

Fig. 6. Impedance behavior of cells in different Li-ion batteries containing: (a) three new, matched cells; (b) six matched, calendar-aged cells; (c) five matched, calendar-aged cells and one overdischarged cell; and (d) five matched, calendar-aged cells [same as in Fig. 6(c)] and one overcharged cell. Each data point in the figure consists of amplitude and phase shift values measured at an individual frequency. The high-frequency *X*-axis intercepts represent the electrolyte resistance, R_s. In Fig. 6(d), data points for cells 4–9 are grouped together near the origin (at the selected axes scales).

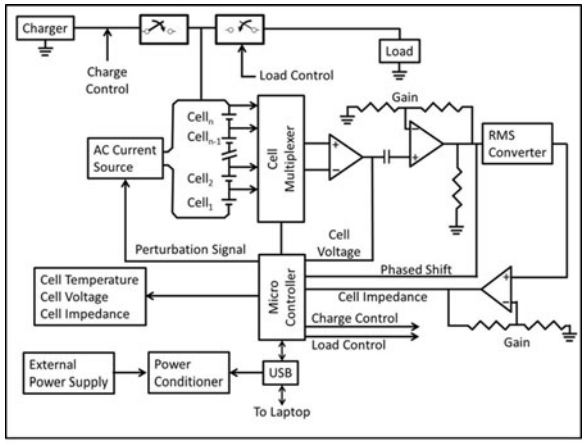

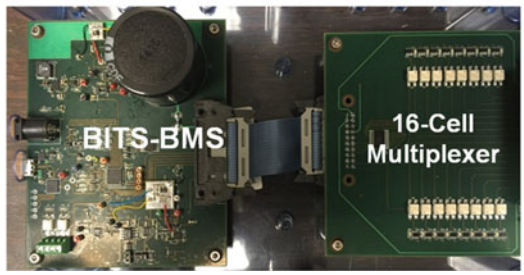

Fig. 7. Impedance-based BMS: schematic describing the main components (top); and photo of the fully operational prototype and a 16-cell multiplexer (bottom). The 10 × 10 cm BMS measures in each cell its anode temperature (at 70 Hz), cathode temperature (10 Hz), electrolyte resistance (400 Hz to 1 kHz), SoC, state of health (SOH) and cell voltage (E_{cv}), while the battery is in use (charge and discharge) or at rest.

SoC, rested overnight before measuring the impedance of the individual cells. Individual cell's impedance drifted from its original value by more than 6% [see Fig. 6(b)], while the spread in impedance values after aging also increased.

We also examined two modified six-cell batteries that had five cells aged as the ones in Fig. 6(b), with the sixth cell replaced by an overdischarged cell, or by an overcharged cell, respectively. The overdischarge protocol involved two cycles of discharge–charge at C/2 rate with an upper cell voltage limit of 4.2 V and a lower cell voltage limit 0.01 V. The nominal lower cell voltage limit for discharge for the cell model used (Swing 5300) is 2.7 V. Similar to most commercial Li-ion cells, the Swing 5300 cell has a copper current collector at the anode. Recharging the cell after discharging it to 0.01 V would generate copper particulates, a type of FOD, which would lead to internal short after several more charge–discharge cycles. The purpose of deliberately overdischarging one cell in the six-cell battery is to demonstrate: 1) cell voltage monitors are unable to identify an overdischarged cell in the battery; and 2) impedance technique can identify the overdischarged cell event, before the event causes internal short.

The impedance of the overdischarged cell after resting the cell overnight at 50% SoC compared to the impedance of the five "normal" aged cells is markedly different [see Fig. 6(c)]. Fig. 6(d) shows impedance data for all six cells in the battery with one cell overcharged twice by charging up to 4.6 V (4.2 V is the upper limit for normal charge). The impedance of the overdischarged cell is 100 000 times larger than the rest of the cells.

V. Impedance-Based BMS

Commercial impedance meters have a wide range of capabilities, but they are rarely used as BMS. Besides size, weight, and power-consumption, they are not designed to monitor simultaneously multiple cells in a battery. Furthermore, conventional BMS that monitor impedance measure only its amplitude at a single frequency, typically at 1 kHz, and are therefore not suitable for properly characterizing a cell mismatch. The data in Fig. 6 demonstrate that cell impedance is indicative of calendar aging, overdischarging, and overcharging. We emphasize that characterizing the impedance of a cell requires amplitude and phase measurements at multiple frequencies. Our impedance-based BMS is designed for such measurements.

We have designed an impedance-based BMS with physical dimensions and power requirements comparable to existing BMS, and with capability to handle batteries with multiple cells, with low or high voltage and Ah-capacity. For example, the data (see Fig. 6) were collected using a bench-top instrument (Solartron). For the same set of batteries, our impedance-based BMS performed as well as the bench-top impedance meter. Measurements were performed in seconds with the batteries both in operation and at rest.

Fig. 7 shows our impedance-based BMS. We call it Battery Internal Temperature Sensor-based BMS, or BITS-BMS. It is designed to monitor each of up to 16 cells in a multicell battery that generates up to 80 V and 50 Ah, with no limit on the battery discharge–charge rates. This 10 × 10 cm unit, powered by a 6 V, 0.75 A dc power supply, is a "standalone" unit, i.e., requires no computer control to operate. It is "ON" when the power supply is "ON," when it starts collecting data for each cell through a 16-cell multiplexer.

A. BITS-BMS Operating Principle

The BITS-BMS collects impedance data by injecting a small-amplitude ac current signal of fixed amplitude (typically 100 mA rms for a 50 Ah cell; or 25 mA rms for a 5 Ah cell) at multiple frequencies in the 1 Hz to 1 kHz range. This ac signal is generated via a programmable microcontroller outputting sinusoidal waveforms of fixed frequencies and fixed amplitude through a current pump. The ac current from the pump is directed toward the cells through the multiplexer, one cell at a time. The ac current perturbs the cell eliciting a voltage response. The BMS generates the perturbation signal through a constant-current source, thus ensuring identical amplitude current passes through each cell in the battery. At each frequency, the circuits following the multiplexer measure the amplitude of the resulting voltage and phase shift between the current and the voltage. The voltage amplitude is a direct measure of the cell impedance, and the phase shift is correlated to the anode temperature and cathode temperature through relationships already discussed in the literature [21], [22]. The BMS has no restriction for the lower frequency cut-off. The 1 Hz to 1 kHz range adequately covers all measurements needed to manage the electrical efficiency and thermal safety in most Li-ion batteries. Each frequency or frequency range in the BMS provides specific information: 70 Hz for the anode temperature; 10 Hz for the cathode temperature; 400–1000 Hz for electrolyte resistance and SOH; and 2 Hz for SoC [21], [23]. Electrolyte resistance is a ratio of cell voltage to the perturbation current, and it is measured by the BMS at a high-frequency [400 Hz in the example shown in Fig. 5(a)].

The BITS-BMS is also equipped to measure and report individual cell voltages. It rosters from one cell to the next through the multiplexer, and the measurement and reporting time per cell for all the parameters is about 22 s. It has two separate features for data processing and utilization. It is programmable to send commands to control systems that regulate the current and voltages in the charging and load circuits. The user can set the desired limits on all parameters, including anode temperature, cathode temperature, cell voltage, internal resistance, SOH, and SoC of each cell. The data can also be sent from the BITS-BMS to a computer for analysis, although a computer is not required to run the BMS.

The BITS-BMS will not short the wirings in the cell and the battery, and battery voltage and currents cannot influence the BMS. The upper battery voltage limit is 80 V that the BMS can handle. It can be redesigned for batteries containing more than 16 cells in series (and therefore having a higher voltage).

B. BITS-BMS Output

BITS-BMS measures ac impedance at multiple frequencies as well as dc volts for E_{cv}. Between 400 Hz and 1 kHz, it measures the amplitude of the resultant ac voltage to an applied ac current, which is converted to electrolyte resistance (R_s, further correlated to SOH). It also measures the impedance at a low frequency (between 1 and 2 Hz) that is correlated to SoC. The amplitude of the resultant ac voltage is measured with a 12-bit analog-to-digital converter (ADC). This binary number is sent to a processor where it is then converted into an impedance value in units of Ohms.

The anode temperature and cathode temperature are measured differently from R_s and SoC. Between 20 and 200 Hz, the BITS-BMS measures the phase shift that is then correlated to anode temperature. At about 10 Hz, it measures the phase shift that is then correlated to cathode temperature. Phase shifts (for example, at 70 and 10 Hz) are measured by comparing the zero crossing of a reference signal with the zero crossing of the return signal from the cell. The frequency of the reference signal is the same as the frequency of the perturbation current. The time interval between the zero-crossing of these two signals represents the phase difference between the perturbation signal and the resultant signal across the cell. The time interval is measured by starting and stopping a 16-bit counter which is incremented every 490 nS. For 70 Hz, this yields a phase resolution of 0.0123° per count. The value in the counter is read, added to an accumulator, and then reset for the next measurement. After 64 readings of the counter are accumulated, an average is computed and the result is transmitted to an external computer (via USB), where it is displayed in units of "BITS-BMS Counts" (an arbitrary unit). Each cell model needs to be calibrated at least once against the BITS-BMS Counts (for example, at 70 and 10 Hz for measuring anode temperature and cathode temperature, respectively). During calibration, the relationship between cell temperature and the count is used to determine a fitting function that is then used to convert the counts into units of degrees Celsius. The cell voltage is also measured with the same 12-bit ADC, the resulting binary value is sent to a processor, where it is converted into units of Volts.

In the context of an autonomous BITS-BMS it is not necessary to perform any conversion from the BITS-BMS internal digital values to engineering units (i.e., temperature, voltage, or ohms) but to simply use the internal digital values to make operational decisions (e.g., disconnect load, reduce or shutdown charging current).

VI. Applications of the Newly Designed Impedance-Based BMS

Our impedance-based BITS-BMS has the ability to monitor internal temperatures (anode and cathode) in each cell, and to identify existing and emerging mismatches between cells, independent of whether the battery is at rest, being charged, or supporting a load. Such capabilities are essential to ensure safety because rising internal temperature is a precursor to thermal runaway that usually originate in a single cell (before spreading to the neighboring cell and causing conflagration). Furthermore, rising temperature in a cell skews its electrolyte resistance (high frequency), anode impedance (intermediate frequency), and/or cathode impedance (low frequency), sufficient to cause cell mismatch. The temperature monitoring capabilities of similar BMS have been extensively reported in the literature [11], [12], [20]–[23]. Additional BITS-BMS features are discussed below.

The BITS-BMS is specifically designed to fulfill the essential safety functions, namely, monitor cell matching and SOH, and guard against excursions in T_{int} and E_{cv} outside prespecified

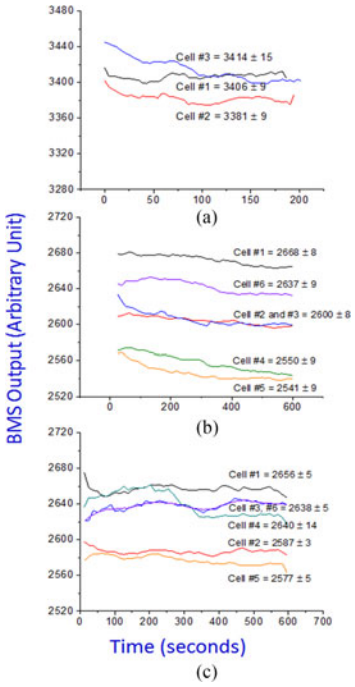

Fig. 8. Outputs of our impedance-based BITS-BMS measured while the batteries are at rest, for: (a) three-cell battery with all new and matched cells (matched within ±0.5%); (b) six-cell battery with originally matched, and then calendar-aged cells (diverged by ±2%); and (c) six cell battery with five calendar-aged cells and one overdischarged cell (Cell #3) (diverged by ±2%).

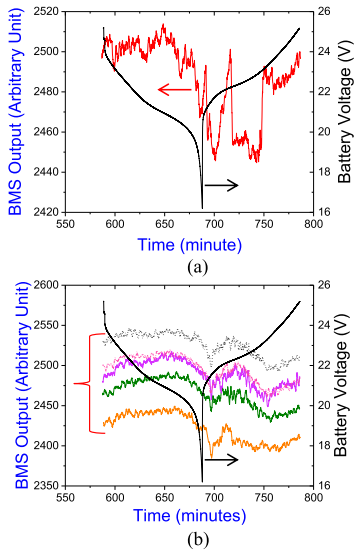

Fig. 9. Outputs of our impedance-based BITS-BMS for a six-cell battery containing five calendar-aged cells and one over-discharged cell, during a discharge–charge cycle: (a) Overdischarged cell only; and (b) five calendar-aged, otherwise normal cells.

safe ranges, for every cell in a battery. In Li-ion cells, unsafe conditions such as thermal runaway are known to develop over a timescale of seconds. Therefore, we designed the BITS-BMS to have short reaction time. Currently, the BITS-BMS monitors safety parameters in each cell with a dwell time not exceeding 22 s, monitoring only R_s (at 400 Hz), anode and cathode temperatures (at 70 and 10 Hz, respectively) and $E_{\rm cv}$. Measurements at different frequencies are sequential, monitoring only the amplitude at 400 Hz, and phase shifts at 70 and 10 Hz.

Measurement of internal temperatures (anode, cathode, and electrolyte) requires calibrating the BITS-BMS output against temperature; such calibration should be performed once for each cell model [21], [22]. For example, the anode temperature in Fig. 3, and the electrolyte temperature in Fig. 5(b) were collected using the calibrated BITS-BMS. $E_{\rm cv}$ measurements (e.g., Fig. 1) need no calibration.

The BITS-BMS outputs the data in binary format. For obtaining calibrated correlation between the binary output and internal temperatures, impedance, etc., the outputs are transferred to a computer through a USB port. For routine purposes of cell matching, controlling the charge and discharge circuits by setting upper and lower limits on the anode and cathode temperature, impedance and cell voltages, the binary outputs of the BITS-BMS are used. We have typically used the binary BITS-BMS outputs (in arbitrary units, Figs. 8 and 9) to identify cell matching in new cells, divergences from matched values (e.g., caused by calendar aging), and mismatching caused by overdischarging.

Fig. 8 shows the outputs of our BMS for multicell batteries with new and matched cells [see Fig. 8(a)], calendar-aged cells [see Fig. 8(b)], and overdischarged cell [see Fig. 8(c)], measured when the batteries were at rest under ambient conditions (21 °C). For all new and matched cells [see Fig. 8(a)], the outputs matched within ±0.5%. We observed a deviation of ±2% among the six cells in the battery with calendar-aged cells [see Fig. 8(b)]. The output of the battery with five aged cells and one overdischarged cell [see Fig. 8(c)] was similar to the one in Fig. 8(b) (six aged cells, but no overdischarged cells). Our impedance-based BMS used for a battery at rest categorized the overdischarged cell as yet another aged cell.

The BITS-BMS outputs during (dis)charge of the battery with five aged cells and one overdischarged cell are shown in Fig. 9. For the five cells, the rates of change of the BMS output were nearly identical; and the absolute values were similar to those for a battery at rest [see Fig. 8(b)]. The trends in the BITS-BMS output for the aged cells under discharge and charge are normal and comparable to those reported earlier [20]. Only the overdischarged cell showed a clear and significant departure in the rate of change of the BMS output, indicative of the cell being bad.

VII. Conclusion

Most conventional BMS monitor parameters (e.g., $E_{\rm cv}$, $T_{\rm surf}$, and R_s at a single frequency) fail to provide safety-relevant information. Our tests showed that $E_{\rm cv}$, $T_{\rm surf}$ and R_s are not indicators for aging or overdischarge-induced cell mismatches.

An impedance-based BITS-BMS, described here, that measures amplitude and phase shift at multiple frequencies (1 to 1000 Hz) is versatile, and can identify safety-relevant characteristics associated with anode, cathode, and electrolyte malfunction [21]. Traditionally, such multifrequency BMS are large and require high electric power to operate, therefore have not spread. Portable BMS that measure impedance do so at a fixed single frequency. These single-frequency measurements are also limited to measuring either the real or quadrature (imaginary)

component [14]–[17]. Here, we demonstrate a small-size, low-power, standalone BMS that is enabled by multifrequency (1–1000 Hz) impedance meter that has phase and amplitude monitoring capability. This BITS-BMS enables battery operation within a user-set range (internal temperature, cell voltage, etc.) and communicates with control systems to regulate charge and discharge currents. The BITS-BMS can successfully identify cell mismatch, and manage thermal safety and electrical efficiency in Li-ion batteries with multiple cells by nearly simultaneously monitoring internal temperature, E_{cv} and R_s in each cell.

References

[1] W. Taylor, G. Krithivasan, and J. J. Nelson, "System safety and ISO 26262 compliance for automotive lithium-ion batteries," in *Proc. IEEE Symp. Product Compliance Eng. Proc.*, 2012, pp. 1–6.

[2] S. Dey, S. Mohon, P. Pisu, and B. Ayalew, "Sensor fault detection, isolation, and estimation in lithium-ion batteries," *IEEE Trans. Control Syst. Technol.*, vol. 24, no. 6, pp. 2141–2149, Nov. 2016, doi: 10.1109/TCST.2016.2538200.

[3] M. Giegerich *et al.*, "Open, flexible and extensible battery management system," in *Proc. IEEE 25th Int. Symp. Ind. Electron.*, 2016, pp. 991–996, doi: 978-1-5090-0873-5/16.

[4] W. Waag, C. Fleischer, and D. U. Sauer, "Critical review of the methods for monitoring of lithium-ion batteries in electric and hybrid vehicles," *J. Power Sources*, vol. 258, pp. 321–339, Jul. 2014, doi: 10.1016/j.jpowsour.2014.02.064.

[5] D. Linden and T. B. Reddy, *Handbook of Batteries*, 3rd ed. New York, NY, USA: McGraw-Hill, 2002, ch. 2, pp. 2.1–2.3.

[6] T. Osaka, D. Mukoyama, and H. Nara, "Review—Development of diagnostic process for commercially available batteries, especially lithium ion battery, by electrochemical impedance spectroscopy," *J. Electrochem. Soc.*, vol. 162, no. 14, pp. A2529–A2537, Oct. 2015, doi: 10.1149/2.0141514jes.

[7] National Aeronautics and Space Administration, Houston, TX, USA, "Cell matching," in *Crewed Space Vehicle Battery Safety Requirements*, Jan. 2014, Sec. 4.4.4, p. 19.

[8] Naval Sea Systems Command, Washington, DC, USA, "Lithium battery system design," in *Technical Manual for Batteries, Navy Lithium Safety Program Responsibilities and Procedures*, S9310-AQ-SAF-010, Oct. 2010, ch. 4.

[9] P. Suresh, A. K. Shukla, and N. Munichandraia, "Temperature dependence studies of a.c. impedance of lithium-ion cells," *J. Appl. Electrochem.*, vol. 32, pp. 267–273, Mar. 2002.

[10] S. S. Zhang, K. Xu, and T. R. Jow, "Electrochemical impedance study on the low temperature of Li-ion batteries," *Electrochim. Acta*, vol. 49, no. 7, pp. 1057–1061, 2004, doi: 10.1016/j.electacta.2003.10.016.

[11] R. Srinivasan *et al.*, "The five modes of heat generation in a Li-Ion cell under discharge," *J. Power Sources*, vol. 262, pp. 93–103, Sep. 2014, doi: 10.1016/j.jpowsour.2014.03.062.

[12] R. Srinivasan and B. G. Carkhuff, "Empirical analysis of contributing factors to heating in lithium-ion cells: Anode entropy versus internal resistance," *J. Power Sources*, vol. 241, pp. 560–566, Nov. 2013, doi: 10.1016/j.jpowsour.2013.04.108.

[13] [Online]. Available: http://gizmodo.com/this-is-why-you-should-take-lithium-ion-battery-fires-v-1788281947. Accessed on: Jan. 12, 2018.

[14] L. H. J. Raijmakers, D. L. Danilov, J. P. M. van Lammeren, T. J. G. Lammers, H. Jan Bergveld, and P. H. L. Notten, "Non-zero intercept frequency: An accurate method to determine the integral temperature of Li-Ion batteries," *IEEE Trans. Ind. Electron.*, vol. 63, no. 5, pp. 3168–3178, May 2016, doi: 10.1109/TIE.2016.2516961.

[15] J. P. Schmidt, S. Arnold, A. Loges, D. Werner, T. Wetzel, and E. Ivers-Tiffée, "Measurement of the internal cell temperature via impedance: Evaluation and application of a new method," *J. Power Sources*, vol. 243, pp. 110–117, Dec. 2013, doi: 10.1016/j.jpowsour.2013.06.013.

[16] N. S. Spinner, C. T. Love, S. L. Rose-Pehrsson, and S. G. Tuttle, "Expanding the operational limits of the single-point impedance diagnostic for internal temperature monitoring of lithium-ion batteries," *Electrochim. Acta*, vol. 174, pp. 488–493, Aug. 2015, doi: 10.1016/j.electacta.2015.06.003.

[17] C. T. Love and K. Swider-Lyons, "Battery health monitoring system and method," U.S. Patent 9465077, Oct. 11, 2016.

[18] S. Bae, H. D. Song, I. Nam, G.-P. Kim, J. M. Lee, and J. Yi, "Quantitative performance analysis of graphite-LiFePO4 battery working at low temperature," *Chem. Eng. Sci.*, vol. 118, pp. 74–82, Oct. 2014, doi: 10.1016/j.ces.2014.07.042.

[19] J. C. Forman, S. J. Moura, J. L. Stein, and H. K. Fathy, "Genetic identification and fisher identifiability analysis of the Doyle–Fuller–Newman model from experimental cycling of a LiFePO4 cell," *J. Power Sources*, vol. 210, pp. 263–275, Jul. 2012, doi: 10.1016/j.jpowsour.2012.03.009.

[20] R. Srinivasan, "Monitoring dynamic thermal behavior of the carbon anode in a lithium-ion cell using a four-probe technique," *J. Power Sources*, vol. 198, pp. 351–358, Jan. 2012, doi: 10.1016/j.jpowsour.2011.09.077.

[21] R. Srinivasan *et al.*, "Instantaneous measurement of the internal temperature in lithium-ion rechargeable cells," *Electrochim. Acta*, vol. 56, no. 17, pp. 6198–6204, Jul. 2011, doi: 10.1016/j.electacta.2011.03.136.

[22] R. Srinivasan and L. Srinivasan, "Graphite carbon anode temperature reflects crystallographic phase transitions in lithium-ion cells," *J. Power Sources*, vol. 293, pp. 876–882, Oct. 2015, doi: 10.1016/j.jpowsour.2015.06.017.

[23] U.S. Patents 8961004 and US 9331507 and International Patents WO 2012054473A1; EP 2630687.

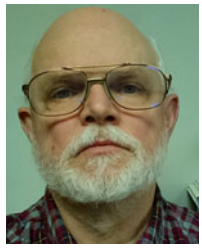

Bliss G. Carkhuff received the B.S. and M.S. degrees from Johns Hopkins University, Laurel, MD, USA, in 1997 and 2011, respectively in electrical engineering.

He is a Principal Staff Member with the Johns Hopkins University Applied Physics Laboratory. He has been on staff with the Applied Physics Laboratory since 1983, supporting projects in the areas of biomedical implants, satellite systems, ocean engineering, transportation infrastructure monitoring, and stratospheric balloon missions for both solar physics and planetary sciences. His current work includes developing sensor systems for biomechanical surrogates and battery safety sensors.

Plamen A. Demirev received the M.S. degree in physics and the Ph.D. degree in chemistry from the University of Sofia and the Bulgarian Academy of Sciences, Sofia, Bulgaria, in 1979 and 1988, respectively.

He is a Principal Staff Member of the Johns Hopkins University Applied Physics Laboratory, Laurel, MD, USA. From 1990 to 1998, he was on the faculty of Uppsala University, Uppsala, Sweden, working on ion-solid and laser-solid interactions. His current research interests include physical methods and sensors for rapid detection of chemicals and pathogens in complex environments.

Rengaswamy Srinivasan received the M.S. degree in chemistry from Banaras Hindu University, Varanasi, India, in 1974, and the Ph.D. degree in chemistry from the Indian Institute of Science, Bengaluru, India, in 1978.

He is a Principal Staff Member with the Johns Hopkins University Applied Physics Laboratory, Laurel, MD, USA. From 1978 to 1983, he was a member of the faculty at the Indian Institute of Technology, Bombay, India. His current research interests include electrochemical sensors, corrosion, and battery safety.

Dr. Srinivasan is the Cochair of the American Institute of Aeronautics and Astronautics Space System Battery Safety Committee on Standards, and an active member of the Battery Safety Council, National Transportation Safety Board, USA.